The magnetic order of $GdMn_2Ge_2$ studied by neutron diffraction and x-ray resonant magnetic scattering

2010 J. Phys.: Condens. Matter 22 226005

(http://iopscience.iop.org/0953-8984/22/22/226005)

J. Phys.: Condens. Matter **22** (2010) 226005 (6pp) doi:10.1088/0953-8984/22/22/226005

The magnetic order of $GdMn_2Ge_2$ studied by neutron diffraction and x-ray resonant magnetic scattering

S A Granovsky[1,2], A Kreyssig[3], M Doerr[2], C Ritter[4], E Dudzik[5], R Feyerherm[5], P C Canfield[3] and M Loewenhaupt[2]

[1] M V Lomonosov Moscow State University, 119991 GSP-1 Moscow, Russia
[2] TU Dresden, Institut für Festkörperphysik, D-01062, Dresden, Germany
[3] Ames Laboratory USDOE, Iowa State University, Ames, IA 50011, USA
[4] Institut Laue-Langevin, F-38042 Grenoble Cedex 9, France
[5] Helmholtz-Zentrum Berlin für Materialien und Energie GmbH, BESSY, D-12489, Berlin, Germany

E-mail: ser@plms.ru

Received 18 February 2010, in final form 28 April 2010
Published 20 May 2010
Online at stacks.iop.org/JPhysCM/22/226005

Abstract
The magnetic structure of $GdMn_2Ge_2$ (tetragonal $I4/mmm$) has been studied by hot neutron powder diffraction and x-ray resonant magnetic scattering techniques. These measurements, along with the results of bulk experiments, confirm the collinear ferrimagnetic structure with moment direction parallel to the c-axis below $T_C = 96$ K and the collinear antiferromagnetic phase in the temperature region $T_C < T < T_N = 365$ K. In the antiferromagnetic phase, x-ray resonant magnetic scattering has been detected at Mn K and Gd L_2 absorption edges. The Gd contribution is a result of an induced Gd 5d electron polarization caused by the antiferromagnetic order of Mn-moments.

(Some figures in this article are in colour only in the electronic version)

1. Introduction

Among the large variety of magnetic materials containing rare earth and 3d elements, the ternary RT_2X_2 compounds (R = rare earth or Y, T = transition metal, X = Ge or Si) are of special interest. These compounds exhibit a wide range of physical phenomena: superconductivity, mixed valence, Kondo and heavy-fermion behavior. Whereas RT_2X_2 compounds with T = Co, Fe and Ni have non-magnetic 3d sublattices, the magnetic properties of manganese containing RMn_2X_2 are determined by two subsystems formed by rare earth and manganese ions. Various magnetic structures and a number of field-, temperature- or pressure-induced magnetic phase transitions were observed in these compounds due to the interplay between the exchange interactions of the different subsystems [1].

RT_2X_2 compounds crystallize in the $ThCr_2Si_2$ type tetragonal structure (space group $I4/mmm$) [2]. The R, T = Mn and X layers form a sequence R–X–Mn–X–R along the tetragonal axis. The Mn-atoms occupy a primitive tetragonal sublattice in this structure in which the distance between the Mn-atoms in the layer is approximately half the distance between the adjacent Mn-layers. This feature leads to a significant spread of the manganese 3d electrons within the layers, and, as a result, to a significant dependence of the strength and of the sign of magnetic interactions on the intra-layer Mn–Mn distances [3]. Investigations made on numerous $(R_1, R_2)Mn_2Ge_2$ compounds with non-magnetic rare earths R_1 and R_2 showed a universal dependence of the magnetic order on the distance between Mn ions in the layer. Below T_N and in the absence of a magnetically ordered R-sublattice, the Mn-moments are forced to couple collinearly antiparallel for intra-layer Mn–Mn distance less than a critical value $d_C \approx 2.83$ Å. For distances between 2.83 Å $< d <$ 2.89 Å the ground state is a non-collinear antiferromagnetic order. However, phase transitions to non-collinear ferromagnetic or conical phases occur at higher temperatures. Compounds with $d > 2.85$ Å exhibit a sequence

of phase transitions with increasing temperature first from non-collinear antiferromagnetic to conical and then to an intra-layer antiferromagnetic phase. Samples with $d > 2.89$ Å have conical magnetic structures at low temperatures [4]. A schematic phase diagram is given by Venturini *et al* [5].

If the rare earth ion R is magnetic, the R–Mn and R–R couplings have to be considered and the competition between Mn–Mn and R–Mn interactions determines the low-temperature properties of RMn_2X_2. As the 4f electrons of the rare earths are localized, the R–Mn coupling is established through hybridization of rare earth 5d and manganese 3d bands [6]. The strength of the R–R exchange in this series of intermetallics is much smaller in comparison to the R–Mn and Mn–Mn couplings [7].

In $GdMn_2Ge_2$ the intra-layer Mn–Mn distance is slightly smaller than d_C at room temperature [5, 8]. According to results of magnetization, resistivity, and thermal expansion experiments, a collinear ferrimagnetic structure with the Gd- and Mn-moments coupled antiparallel along the c-axis, is formed below $T_C = 96$ K [9, 10]. With increasing temperature the strength of the R–Mn exchange is decreasing and at T_C magnetic moments rearrange to an antiferromagnetic structure. The transition ferrimagnetism–antiferromagnetism is of first-order type and is accompanied by a significant lattice expansion ($\Delta V/V \approx 3 \times 10^{-3}$) and an anomaly of the temperature-dependent electrical resistivity. Above T_C the molecular field of the neighboring Mn-atoms in the high-temperature phase is compensated at the Gd sites. Therefore, the Gd-moments do not order in the antiferromagnetic phase and an independent magnetic order of Mn-moments is established in this temperature region up to the Néel temperature $T_N = 365$ K.

As for most compounds containing strongly neutron-absorbing elements, conclusions about the type of magnetic order in $GdMn_2Ge_2$ have been deduced from bulk data. However, there is controversy in the results published by different authors. In [11] a non-collinear antiferromagnetic structure with a moment component perpendicular to the c-axis is proposed for the temperature region between T_C and T_N while other authors claim a collinear antiferromagnetic state [9, 10]. There is still an open question about the existence of a high-temperature weakly ferromagnetic phase above T_N. Dilatometry data on $GdMn_2Ge_2$ show that this compound may overcome the critical value d_C at high temperatures due to thermal expansion [12]. In this case an additional magnetic phase transition may take place. The observation of this transition was reported in [8, 13]—an additional kink in the thermal dependence of magnetization and resistivity was detected at $T^* \approx 480$ K. X-ray thermal expansion measurements were also performed; however, the accuracy of this experiment was not enough to prove or to deny the existence of this high-temperature phase [12]. Therefore, microscopic experiments are of particular importance to clarify the magnetic properties of $GdMn_2Ge_2$. High-intensity hot neutron and synchrotron radiation sources allow us to investigate magnetic structures of neutron-absorbing materials using the combination of hot neutron powder diffraction and x-ray resonant magnetic scattering (XRMS). Thus, the well quantifiable magnetic scattering in a neutron experiment can be combined with the good angular resolution of the XRMS technique. In this paper the study of the magnetic structure in $GdMn_2Ge_2$ obtained by these two complementary methods is reported.

2. Experimental details

An 8 g polycrystalline sample of $GdMn_2Ge_2$ was synthesized from elements with at least 99.9% purity in an induction furnace using a quasi-levitation copper crucible. A 2 wt% excess of Mn was added to the stoichiometric mixture in order to compensate the preferential Mn evaporation during the melting procedure. To ensure the homogeneity, the ingot was remelted three times in high-purity Ar atmosphere and then annealed in dynamic vacuum at 850 °C for 120 h. X-ray powder diffraction analysis showed the $ThCr_2Si_2$ phase to be present as the main phase (not less than 95 vol%). For the XRMS experiment we used a single crystal of $GdMn_2Ge_2$ out of the same batch used in [14] grown by the flux method as described in [15]. Both samples were made from a natural isotope-mixture of Gd.

The low-field AC magnetic susceptibility, χ_{AC}, was measured by an induction method in a magnetic field of $H_{AC} = 15$ Oe. The electrical resistivity, ρ, measurements were carried out by a standard four-probe method using silver paint to fix the contacts. $\rho(T)$ measurements were limited to the stability range of the conducting paint $T \leqslant 420$ K. Magnetization versus temperature was measured in the temperature range $4\ \text{K} < T < 600$ K in an Oxford vibrating sample magnetometer equipped with the high-temperature furnace insert.

Neutron diffraction experiments were performed at ILL, Grenoble. Diffractograms were collected at the hot source powder and liquid diffractometer D4. The neutron wavelength was set to $\lambda = 0.4972$ Å using a Ge monochromator. Diffraction patterns were collected at different temperatures with a counting time of 2 h/pattern. To cover the whole temperature range of magnetic phase transitions an orange-type cryostat ($4\ \text{K} < T < 300$ K) was used together with a resistance furnace ($300\ \text{K} < T < 600$ K). For both sample environments the background scattering was determined by measuring an empty sample container and the same container filled with strongly absorbing enriched ^{10}B powder. A linear combination of both measured backgrounds was then subtracted from the measured scattering intensity in order to give the purely sample determined scattering. The so-corrected neutron diffraction patterns were analyzed by a modified Rietveld method using the FULLPROF software [16]. The effective coherent cross-section of the natural Gd was set to 9.3 fm in the refinements [17].

The XRMS experiment was performed at the MAGS beamline at BESSY, Berlin. The sample with its surface perpendicular to the (001) direction was mounted on the cooper head of the closed-cycle displex refrigerator. Scans were performed in the vertical ($\sigma - \pi$) scattering geometry using a graphite analyzer.

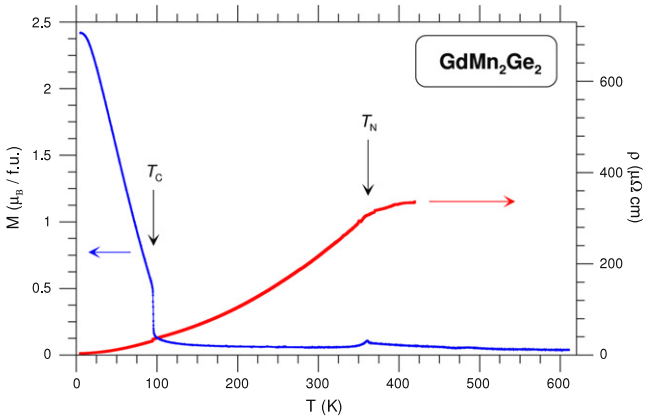

Figure 1. Temperature dependence of the magnetization for polycrystalline $GdMn_2Ge_2$ measured in a magnetic field $B = 0.7$ T. Temperature dependence of the (zero field) electrical resistivity for $GdMn_2Ge_2$.

3. Results and discussion

Macroscopic measurements have been performed to characterize the polycrystalline $GdMn_2Ge_2$ sample. Major results are shown in figure 1. The magnetization versus temperature dependence $M(T)$ indicates the ferrimagnetic behavior below $T_C = 96$ K. On reaching T_C the magnetization sharply decreases and a jump-like increase in the electrical resistivity is observed, indicating a first-order magnetic phase transition. At $T_N = 365$ K, the Néel transformation corresponds to a small kink in $M(T)$ and a negative turn of the $\rho(T)$ dependence. AC-susceptibility data (not shown) confirm the transitions at T_C and T_N. The results of the bulk experiments are in good agreement with previously reported data [8–13].

The XRMS technique was recently employed by Kim *et al* [14] to study the ferrimagnetic phase of $GdMn_2Ge_2$. Analyzing the resonance at the Gd L_2 edge it was proven that Gd-moments are ferromagnetically aligned in the [001] direction below T_C. The present study focuses on XRMS measurements between T_C and T_N. Figure 2 (plots (a) and (b)) shows the energy dependences close to Gd L_2 and Mn K absorption edges for the fluorescence signal and for the intensity of the magnetic (007) reflection obtained at $T = 200$ K. Element-specific resonance enhancements were detected for both Gd and Mn magnetic scattering cross sections.

Rocking scans of the (007) magnetic reflections are shown in figures 2(c) and (d) for selected temperatures between T_C and T_N. In order to allow comparison, the intensities of the XRMS peaks measured at $E^{L2}_{Gd} = 7921.5$ eV and $E^{K}_{Mn} = 6532$ eV are normalized by the intensity of the charge (008) reflections registered under identical experimental conditions. It can be clearly seen that the intensities of the Gd L_2 and the Mn K resonances correlate to each other at all temperatures. The (007) reflection vanishes above $T = 370$ K at both absorption edges. At each temperature the Gd resonance is roughly two orders of magnitude weaker than the Mn resonance and much weaker than in XRMS experiments on GdT_2X_2 compounds with ordered local Gd-moments [18]. We conclude that the observed XRMS signals between T_C and T_N are related to the antiferromagnetic order of the Mn-moments. The nature behind the signal at the Gd L_2 absorption edge will be discussed later.

Numerous other reciprocal lattice points were also examined in order to find magnetic signals, revealing the absence of magnetic scattering elsewhere than at the (hkl) positions where $h + k + l =$ odd and integer. From the polarization condition $(\sigma - \pi)$ for the measured XRMS reflections and the intensity ratios for different magnetic $(00l)$ reflections, we conclude that the magnetic moments are oriented in the c-direction in the high-temperature phase $T_C < T < T_N$. These results are consistent with proposals based on bulk experiments [8–10, 12].

Neutron diffraction patterns were obtained in the temperature range 5 K $< T <$ 573 K. In figure 3, diffraction patterns and their Rietveld analysis are shown at selected temperatures characteristic for different magnetic phases. First the crystal structure was refined in the paramagnetic phase at 573 K. Difference spectra were then used to gain the needed information on the possible adopted magnetic structures by displaying typical magnetic Bragg peaks. By comparison with the high-resolution data for non-absorbing isostructural $TbMn_2Ge_2$ known from the literature, (Tb, Nd)Mn_2Ge_2 and $TbMn_2Si_2$ compounds [19, 20] were used to recognize and construct the specific models used for the magnetic structure refinements. Using the selected model, the values of magnetic moments at Gd and Mn sites were determined.

No evidence of qualitative magnetic structure changes was observed in the temperature range 393 K $< T <$ 573 K. The difference spectrum of diffractograms obtained at 300 and 393 K reveals a weak magnetic contribution to the diffraction peak at $2\theta \approx 10.5°$ associated to the (111) magnetic reflection and the outcome of the magnetic (113) reflection at about $2\theta \approx 12.8°$ (figure 3(b)). At the same time no magnetic contribution to (00 $2n$) reflections is present over the whole temperature range. These observations, together with results of the XRMS experiment lead us to the selection of the collinear antiferromagnetic *AFil* phase model for the temperature range 96 K $< T <$ 365 K (here and below we use the classification for RMn_2X_2 compounds defined in [5]). Below $T_C = 96$ K the significant increase of intensity of the (101) and (211) peaks (figure 3(c)) and the constant intensity of the (002) peak give evidence for the presence of the collinear ferrimagnetic F model at low temperatures.

The temperature dependencies of the Gd and Mn magnetic moments obtained from the Rietveld refinements are shown in figure 4 along with the integrated magnetic intensity of the (007) reflection measured at Gd L_2 and Mn K resonances. Normalized data from [14] are also included for the ferrimagnetic phase.

According to the Rietveld refinement, at 5 K the magnetic moments on the Gd sites, $M_{Gd} = 7.0 \pm 0.2\ \mu_B$, are aligned along the tetragonal c-axis and are opposite in direction to the Mn-moments, $M_{Mn} = 2.1 \pm 0.2\ \mu_B$ so that the collinear ferrimagnetic F structure is established. With increasing temperature, M_{Gd} decreases gradually down to $4.9 \pm 0.2\ \mu_B$ at 90 K while M_{Mn} exhibits no visible change. The magnetic structure corresponds to the one found in $TbMn_2Ge_2$ and in

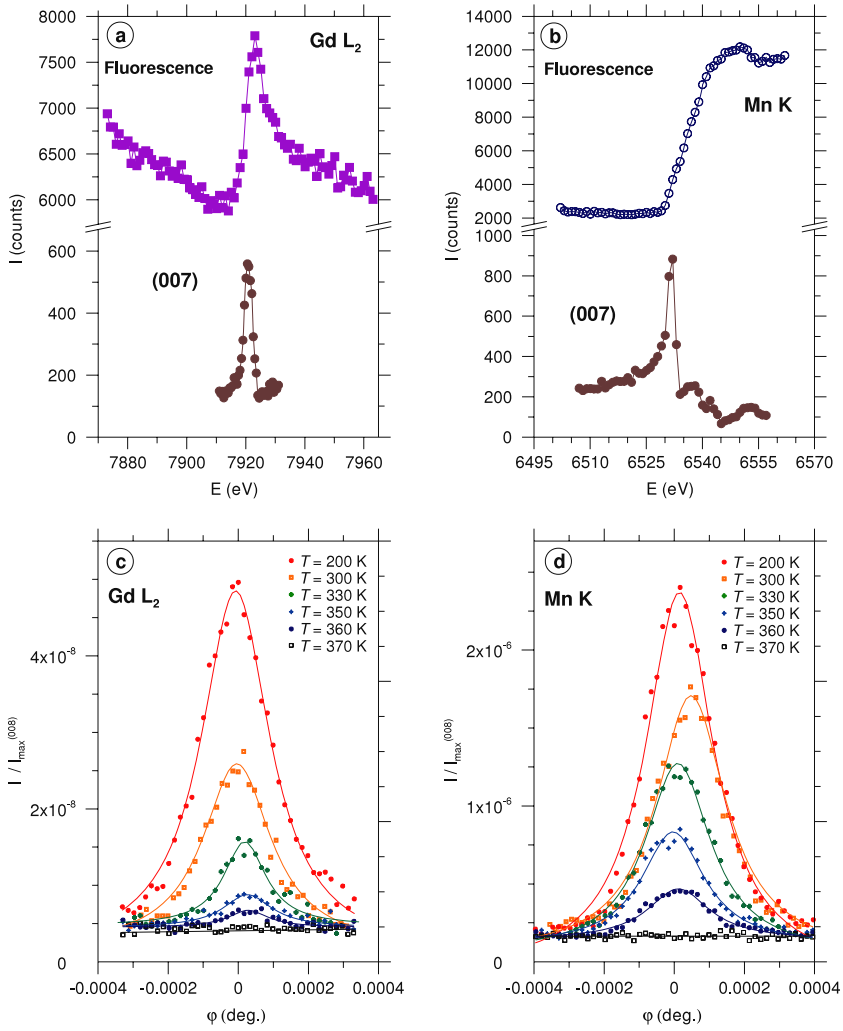

Figure 2. Energy scans through Gd L_2 (a) and Mn K (b) absorption edges. Scans done at $T = 200$ K for the fluorescence (upper parts) and (007) reflection. Rocking scans through the (007) diffraction peak measured at Gd L_2 (c) and Mn K (d) absorption edges for selected temperatures.

the mixed system $Tb_{1-x}Nd_xMn_2Ge_2$ up to about $x = 0.3$ [20]. This is not surprising as the chemical pressure effect induced by replacing the Tb^{3+} ion by the larger Gd^{3+} ion corresponds to the one when substituting about 18% of Tb^{3+} by Nd^{3+}. The relatively low value of the Mn magnetic moment found at 5 K ($M_{Mn} = 2.1 \pm 0.2\ \mu_B$) compares well to those found in $TbMn_2Ge_2$ ($M_{Mn} = 1.7 \pm 0.1\ \mu_B$) and $Tb_{0.8}Nd_{0.2}Mn_2Ge_2$ ($M_{Mn} = 1.8 \pm 0.1\ \mu_B$) where the Mn-sublattice adopts the same ferrimagnetic F structure [20].

In the narrow temperature range 91 K $< T <$ 97 K, M_{Gd} drops to zero and, simultaneously, the magnetic Mn-moments re-align from a parallel to an antiparallel arrangement, so that the resulting magnetic structure of $GdMn_2Ge_2$ at higher temperatures is collinear and antiferromagnetic as in $TbMn_2Ge_2$. There is no sign of an additional antiferromagnetic coupling along the a-axis (magnetic contribution to the (101) peak) as found in $Tb_{0.8}Nd_{0.2}Mn_2Ge_2$ which would be indicative of the *AFmc* type magnetic structure. Our x-ray thermal expansion data [12] had determined the intra-layer distance at 96 K to $d_{Mn-Mn} = 2.833 \pm 0.001$ Å and therefore just below the limit of $d_{Mn-Mn} = 2.84$ Å for which Venturini *et al* [21] determined the onset of an additional antiferromagnetic coupling along the a-axis leading to the *AFmc* type magnetic structure. The best fit gives value $M_{Mn} = 1.9 \pm 0.2\ \mu_B$ at 105 K. M_{Mn} stays nearly constant up to $T = 300$ K before it gradually decreases. Our magnetization and diffraction experiments show that above $T_N = 365$ K $GdMn_2Ge_2$ has no long-range magnetic ordering. Magnetic phase transitions observed near $T^* \approx 480$ K in [8, 13] may originate from ferro- or ferrimagnetic binary or ternary impurities with close composition in the Gd–Mn–Ge phase diagram (for example, Gd_6Mn_{23} is a ferrimagnet with $T_C = 468$ K [22]). Thus, the magnetic behavior of $GdMn_2Ge_2$ is in good agreement with a modified Yafet–Kittel model for a two-sublattice ferrimagnet stated in [23] and with the intra-layer Mn–Mn coupling scheme proposed in [5, 21].

One possible reason for the absence of the additional ferromagnetic phase might be that $GdMn_2Ge_2$ does not overcome the critical distance d_C. Our current results on hot neutron powder diffraction do not have sufficient resolution to enable us to refine the temperature dependence of the lattice parameters. Following the x-ray thermal expansion data [12]

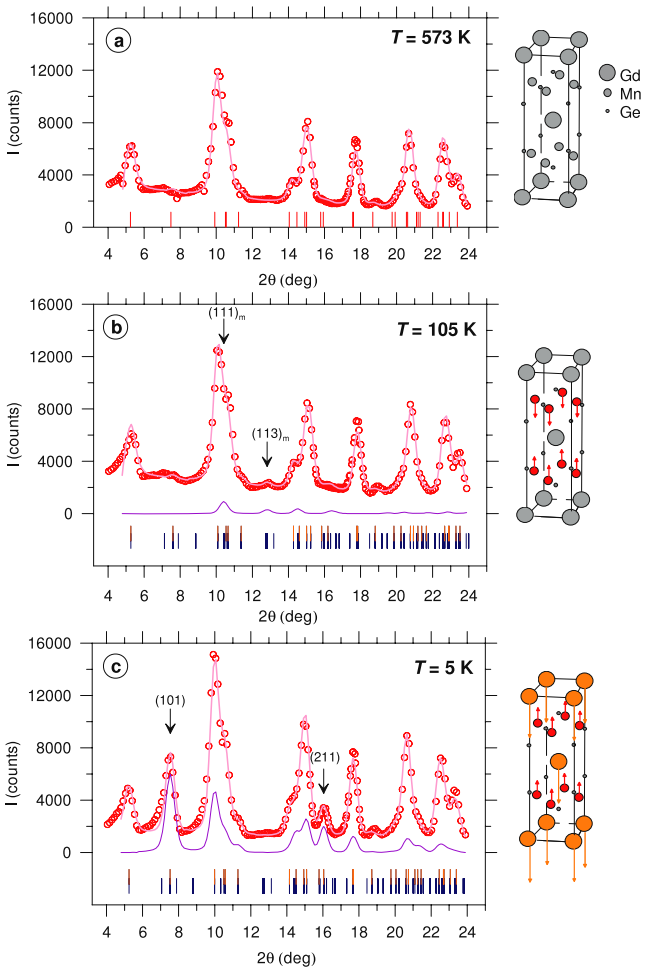

Figure 3. Neutron diffraction patterns of $GdMn_2Ge_2$ at $T = 573$ K (paramagnetic phase) (a), $T = 105$ K (antiferromagnetic phase *AFil*) (b) and $T = 5$ K (ferrimagnetic phase *F*) (c). Points represent the experimental data, lines—the result of the Rietveld refinement for the diffraction pattern and its magnetic part separately (lower lines on (b) and (c)). Bars indicate the reflection positions for the structural and magnetic phases. The schemes illustrate the magnetic structure model used for refinement.

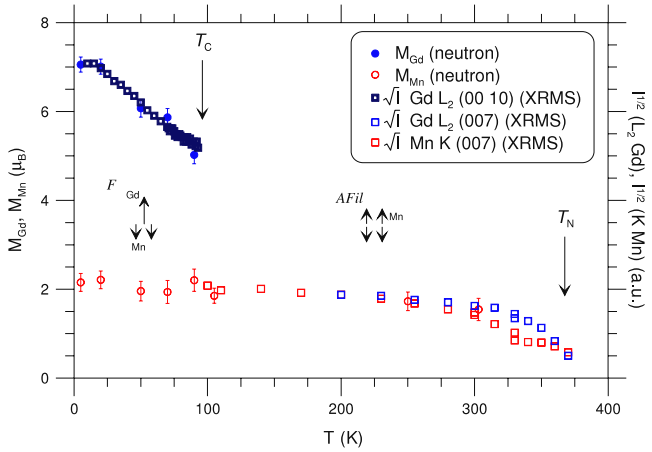

Figure 4. Temperature dependence of Gd and Mn magnetic moments in the ferrimagnetic and antiferromagnetic phases—results of Rietveld refinements of neutron data. Normalized thermal variation of the square root of the measured XRMS intensities—magnetic contribution to the (00 10) peak at the Gd L_2 edge (taken from [14]), temperature dependence of the (007) magnetic peak measured at the Gd L_2 and Mn K absorption edges.

the intra-layer distance is $d^{96\ K}_{Mn-Mn} = 2.833 \pm 0.001$ Å just above T_C and $d^{365\ K}_{Mn-Mn} = 2.849 \pm 0.001$ Å at the Néel point. Both these spacings lie within the range for the collinear antiferromagnetic *AFil* structure (one has to recall here that d_c is temperature dependent and varies between about 2.83 Å at 0 K and 2.85 Å at 350 K [5]). Another explanation could be the influence of the Gd ions on the interlayer Mn–Mn interactions at high temperatures.

The combination of hot neutron diffraction with XRMS proved to be efficient and complimentary to study the complex magnetic order in $GdMn_2Ge_2$. The current work is also of methodical importance. The appearance of resonance scattering at the Gd L_2 edge should not be interpreted as scattering concerned with an ordering of the local Gd (4f) magnetic moments but as resulting from the polarization of the Gd (5d) electrons induced by the Mn order in this particular case. The temperature dependence of the Gd L_2 resonance clearly shows the correlation with the antiferromagnetic ordering of the Mn-sublattice vanishing at $T_N = 365$ K while the neutron diffraction data revealed the absence of Gd magnetic ordering. We can interpret the observed resonance magnetic scattering at the Gd L_2 edge in the following way: the interaction between the band magnetism and the almost localized 4f moments of the rare earth establishes itself through hybridization of the 3d states of the transition metal with the 5d states of the lanthanide and then, through the local exchange, with the 4f moment [6]. Therefore, the long-range magnetic ordering in the Mn-sublattice in $GdMn_2Ge_2$ should affect the Gd-moments. As a result, the spin polarization of the Gd 5d band follows the antiferromagnetic ordering of the Mn-sublattice although the strength of R–Mn interaction is insufficient to establish a Gd long-range ordering of the local 4f Gd-moments. Thus measured resonant enhancements at the Gd L_2 edge result from the spin polarization of the Gd 5d band induced by antiferromagnetic ordering of the Mn-sublattice. This is consistent with the fact that the induced scattering signal at the Gd L_2 edge is roughly two orders of magnitude weaker than the Mn K signal.

Summarizing, the magnetic structure of $GdMn_2Ge_2$ was determined by a combination of hot neutron powder diffraction and XRMS. Below $T_C = 96$ K the magnetic moments of Gd are aligned along the *c*-axis antiparallel to the Mn-moments so that the collinear ferrimagnetic *F* structure is established. In the temperature range 96 K $< T <$ 365 K the Gd-sublattice has no long-range magnetic order and the Mn-moments are aligned collinearly antiparallel to each other (*AFil* structure). An XRMS experiment shows that the antiferromagnetic ordering of the Mn-moments induces enhancements not solely for the Mn K resonance, but, by means of 3d–5d hybridization, also for the resonances at the Gd absorption edges.

Acknowledgments

This work was supported by RFBR (09-02-01475-a) and the Erasmus-Mundus Program of the European Union

(ECW-L04 TUD 08-59). The work by PCC and AK at the Ames Laboratory was supported by US DOE, Office of Science, under contract DE-AC02-07CH11358.

References

[1] Szytula A and Leciejewicz J 1989 *Handbook on the Physics and Chemistry of Rare Earths* vol 12, ed K A Gschneidner Jr and L Eyring (Amsterdam: Elsevier) p 133
[2] Ban Z and Sikirica M 1965 *Acta Crystallogr.* **18** 594
[3] Szytula A 1993 *Int. J. Mod. Phys.* B **7** 859
[4] Venturini G, Malaman B and Ressouche E 1996 *J. Alloys Compounds* **240** 139
[5] Venturini G, Malaman B and Ressouche E 1996 *J. Alloys Compounds* **241** 135
[6] Brooks M S S, Nordström N and Johansson B 1991 *Physica* B **172** 95
[7] Venturini G, Malaman B, Tomala K, Szytula A and Sanchez J P 1992 *Phys. Rev.* B **46** 207
[8] Kervan S, Acet M and Elerman Y 2001 *Solid State Commun.* **119** 95
[9] Guo G, Levitin R Z, Sokolov A Yu, Snegirev V V and Filippov D A 2000 *J. Magn. Magn. Mater.* **214** 301
[10] Wada H, Yoshioka H and Goto T 2002 *J. Phys.: Condens. Matter* **14** 3241
[11] Fujiwara T and Fujii H 2001 *Physica* B **300** 198
[12] Gaidukova I Yu, Guo G, Granovsky S A, Dubenko I S, Levitin R Z, Markosyan A S and Rodimin V E 1999 *Phys. Solid State* **41** 1885
[13] Shigeoka T, Fujii H, Fujiwara H, Yagasaki K and Okamoto Y 1983 *J. Magn. Magn. Mater.* **31–34** 209
[14] Kim J W, Kreyssig A, Ryan P, Mun E, Canfield P C and Goldman A I 2007 *Appl. Phys. Lett.* **90** 202501
[15] Canfield P C and Fisk Z 1992 *Phil. Mag.* B **65** 1117
[16] Rodriguez-Carvajal J 1993 *Physica* B **192** 55
[17] Lynn J E and Seeger P A 1990 *At. Data Nucl. Tables* **44** 191
[18] Good W, Kim J, Goldman A I, Wermeille D, Canfield P C, Cunningham C, Islam Z, Lang J C, Srajer G and Fisher I R 2005 *Phys. Rev.* B **71** 224427
[19] Granovsky S A, Gaidukova I Yu, Doerr M, Loewenhaupt M, Markosyan A S and Ritter C 2007 *Physica* B **391** 79
[20] Morellon L, Algarabel P A, Ibarra M R and Ritter C 1997 *Phys. Rev.* B **55** 12363
[21] Venturini G, Welter R, Ressouche E and Malaman B 1995 *J. Magn. Magn. Mater.* **150** 197
[22] Buschow K H J 1980 *Ferromagnetic Materials* vol 1, ed E P Wohlfarth (Amsterdam: North-Holland) p 297
[23] Sokolov A Yu, Guo G, Granovsky S A, Levitin R Z, Wada H, Shiga M and Goto T 1999 *JETP* **89** 723